Inorganic Chemistry
Cite This: Inorg. Chem. 2019, 58, 4063−4066
Communication
pubs.acs.org/IC

Templating Structural Progessions in Intermetallics: How Chemical Pressure Directs Helix Formation in the Nowotny Chimney Ladders

Erdong Lu and Daniel C. Fredrickson*

Department of Chemistry, University of Wisconsin—Madison, 1101 University Avenue, Madison, Wisconsin 53706, United States

Supporting Information

ABSTRACT: In the structural diversity of intermetallic phases, hierarchies can be perceived relating complex structures to relatively simple parent structures. One example is the Nowotny Chimney Ladder (NCL) series, a family of transition metal−main group (T−E) compounds in which the T sublattices trace out helical channels populated by E-atom helices. A sequence of structures emerges from this arrangement because the spacing along the channels of the E atoms smoothly varies relative to that of the T framework, dictated largely by optimization of the valence-electron concentration. In this Communication, we show how this behavior is anticipated and explained by the Density Functional Theory-Chemical Pressure (DFT-CP) schemes of the NCLs. A CP analysis of the $RuGa_2$ parent structure reveals CP quadrupoles on the Ga atoms (telltale signs of soft atomic motion) that arise from overly short Ru−Ga contacts along one axis and underutilized spaces in the perpendicular directions. In their placement and orientation, the CP quadrupoles highlight a helical path of facile movement for the Ga atoms that avoids further compression of the already strained Ru−Ga contacts. The E atoms of a series of NCLs (in their DFT-optimized geometries) are all found to lie along this helix, with the CP quadrupole character being a persistent feature. In this way, the T sublattice common to the NCLs encodes helical paths by which the E-atom spacing can be varied, creating a mechanism to accommodate electronically driven compositional changes. These results illustrate how CP schemes can be combined with electron-counting rules to create well-defined structural sequences, potentially guiding the discovery of new intermetallic phases.

The art of synthesis, in its highest form, involves the recognition of specific points of reactivity in widely available starting materials that can be used to build molecules of increasing complexity. Such an approach is in stark contrast to the state-of-the-art strategies for designing inorganic solid-state compounds. Methods such as evolutionary algorithms and machine-learning models generally aim for the final crystal structure that will be obtained for a given composition.[1−5] This emphasis on synthetic products, as opposed to patterns of reactivity, aligns well with the expectation that the high temperatures used in traditional solid-state synthesis overwhelm any kinetic effects. However, solid-state chemistry is also rich in tantalizing structural relationships that are suggestive of transformations governed by chemical principles. For example, many complicated structures can be derived (at least conceptually) from variations on simpler ones through distortion, fragmentation, intergrowth, or other rearrangements.[6] The ability to predict the rearrangements offered by different structures would open avenues to new intermetallic chemistry. Here, we will illustrate how in one striking series of phases, the Nowotny Chimney Ladders (NCLs),[7] a full structural sequence can be extrapolated from the atomic packing and electron-counting requirements of a common parent structure, suggesting a more general scheme for anticipating superstructure formation in metals and alloys.

The NCLs are a family of transition metal−main group (T−E) phases known for their helix-within-a-helix motifs (Figure 1):

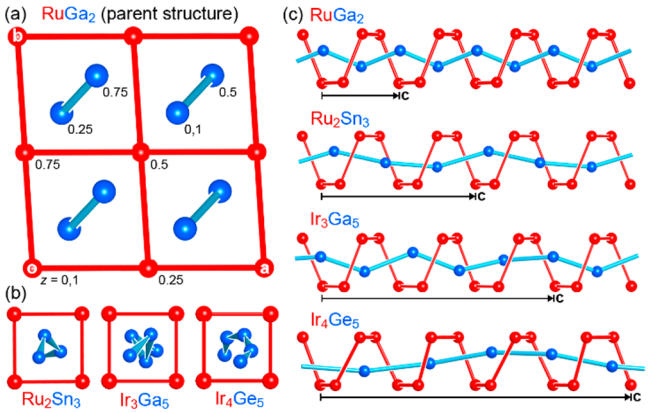

Figure 1. Examples of the NCL phases. (a) $RuGa_2$ ($TiSi_2$ type) parent structure.[11] Helix-within-a-helix motifs of other members shown as (b) top and (c) side views.[12]

the T atoms are arranged into a flattened diamond network (β-Sn type) to form 4-fold helical channels. The E atoms occupy these channels to form a second set of helices that run in a parallel direction, but with a period that is largely decoupled from that of the T atoms. The relative spacing and helicity of the E atoms is determined by the stoichiometry. The composition TE_2 corresponds to the $TiSi_2$-type parent structure (exemplified by $RuGa_2$ in Figure 1a) with one period of the T helix wrapping around exactly two E atoms that belong to a zigzag chain. Longer-period or even incommensurate arrangements[8−10] emerge for more E-atom-poor stoichiometries (TE_{2-x}) as the

Received: January 14, 2019
Published: March 13, 2019

DOI: 10.1021/acs.inorgchem.9b00132
Inorg. Chem. 2019, 58, 4063−4066

helical repeat lengths for the T and E sublattices come out of register with each other.

When the T atoms come from group 7 or higher, these stoichiometries are dictated, sometimes with exquisite precision,[13] to achieve electron concentrations of 14 per T atom, a correlation known as the 14-electron rule.[14−17] Prior theoretical work connected this special electron count to the presence of an electronic band gap or pseudogap at the Fermi energy (E_F) separating filled and empty levels across the series (Figure 2),[16−22] which has helped motivate investigations into the

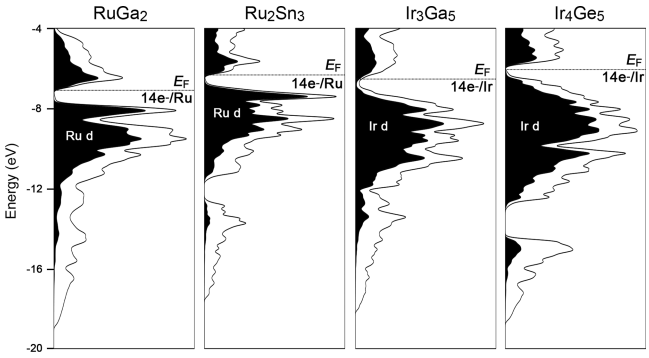

Figure 2. Electronic density of states (DOS, generalized gradient approximation-DFT) distributions for a series of 14-electron NCL structures. The contributions from transition-metal d character are shaded in black. Gaussian broadening has been applied to emphasize the more general features of the curves.

electronic behavior and thermoelectric properties of the NCLs.[20,23−28] The persistence of this stabilizing feature at 14 electrons per T atom was traced to the connectivity of the T-atom sublattice. Here, T@T_4 tetrahedra of the β-Sn-type arrangement allow each T atom to covalently share electron pairs with four T neighbors (supported by bridging interactions with the E atoms). Filled 18-electron configurations are then achieved with only 14 electrons on each T atom,[29] in line with the 18-*n* bonding scheme for T−E intermetallics.[30]

Such a picture makes clear prescriptions for what compositions should be preferred by different T−E combinations: in the Ru−Sn system, reaching 14 electrons per Ru atom requires the composition Ru_2Sn_3, while for the Ir−Ga and Ir−Ge pairings, the dictated stoichiometries are Ir_3Ga_5 and Ir_4Ge_5. However, because the key parameter determining the ideal electron count is the T−T connectivity, the bonding scheme leaves open the question of what arrangement the E atoms should take around the T sublattice. What steers the structure toward helical motifs rather than, say, random E atom vacancies?

Given the dense arrangements usually present in intermetallic phases, a likely candidate is the atomic packing efficiency, i.e., how well the spatial requirements of the atoms are satisfied. The hypothesis that atomic packing factors influence the placement of the E atoms within the NCL structures can be evaluated with the Density Functional Theory-Chemical Pressure (DFT-CP) method,[31−34] in which interatomic pressures arising from geometrical constraints are visualized using the output of electronic structure calculations.

Let us begin with the CP scheme for the parent phase of the 14-electron NCLs, $RuGa_2$, focusing on a single Ru channel and the Ga zigzag chain that it contains (Figure 3a). The local pressures experienced by each atom are represented with radial plots, with the distance from any atomic center to the surface surrounding it being proportional to the sums of the pressure

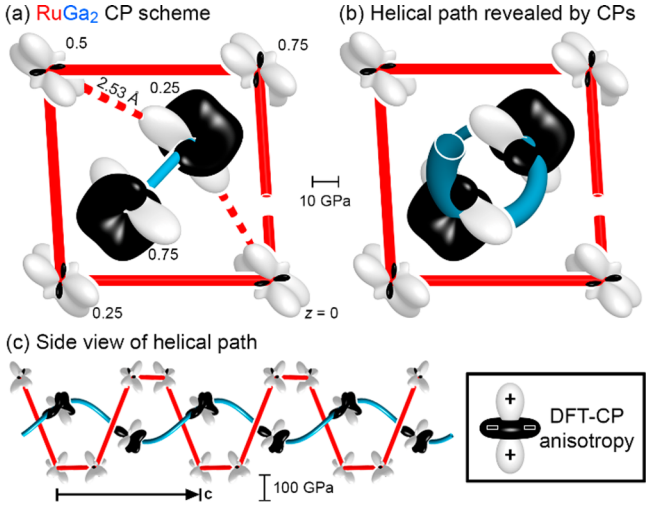

Figure 3. Helicity encoded by the CP scheme of the NCL parent phase $RuGa_2$. (a) CP anisotropies for one channel of the $RuGa_2$ structure, with red dashed lines indicating a set of overly compressed Ru−Ga contacts. (b) Helical path traced out by the Ga CP quadrupoles. (c) Side view of the helical path.

contributions experienced by the atom from that direction. The sign of the pressure is then indicated with color: black portions of the plot correspond to directions of negative pressure, denoting interactions that would be stabilized by the contraction of the structure (too long interatomic distances), while the white features tell of interactions for which expansion of the structure would be favorable (too short interatomic distances). The average of these CPs over the whole structure gives the phase's macroscopic pressure (zero for a geometrically optimized structure).

In Figure 3a, a tension can indeed be perceived between interatomic distances desiring expansion and contraction. The Ru atoms appear with predominantly positive CPs, with white lobes pointing to the nearest-neighbor Ga atoms in the Ru channels. These positive CPs, along the short Ru−Ga contacts, are also reflected in narrow white lobes emanating from the Ga atoms. The remainder of the Ga CPs, however, are negative and diffuse, representing sparse atomic packing along the other directions that prevents the expansion of the structure.

The anisotropic CP distribution around the Ga atoms bears some resemblance to a distorted d_{z^2} orbital, with its pair of positive lobes being directed along one axis and a negative ring wrapping around the equator. Such quadrupolar CP features are strongly indicative of soft atomic motions (as reflected in the vibrational modes or even the emergence of modulations)[35,36] because displacements perpendicular to the positive CPs would both lengthen the overly short distances and lead to denser packing along one direction of negative pressure. Such Ga motions are thus anticipated to be relatively facile. An inspection of the phonon band structure (see the Supporting Information) confirms these expectations.

When we imagine atoms following these paths of negative pressure, an illuminating feature emerges. The placement of each Ga within a 4-fold Ru helix means that its two close Ru neighbors on opposite sides are at different heights, one above and one below (Figure 3a). A tilting of the Ga CP quadrupoles out of the plane of the page results. Because of this tilt, the direction of easy Ga movement runs along the channel, with an angle conforming to twist of the Ru helix. Following this path a

DOI: 10.1021/acs.inorgchem.9b00132
Inorg. Chem. 2019, 58, 4063−4066

little further, in fact, leads us toward the negative CP feature of a neighboring Ga atom within the same Ru channel. Connecting these arcs together between the Ga atoms reveals a helical path along the *c* axis that avoids close Ru−Ga contacts (blue curve in Figure 3b,c) and shares the same repeat period as the Ru helix.

The availability of this continuous route of soft motion provides a simple way by which the stoichiometry of the NCLs can be adjusted in response to electronic requirements. $RuGa_2$ exhibits a band gap at 14 electrons per T atom due to its optimized 18-*n* bonding scheme. Upon moving from the Ru−Ga to Ir−Ga system, an isostructural $IrGa_2$ phase would have one extra electron per Ir atom relative to the ideal count. Restoring the 14-electron count would then necessitate the removal of one Ga atom for every three Ir atoms, leading to the stoichiometry Ir_3Ga_5. Slightly increasing the spacing of the Ga atoms along the helical path of soft motion provides a mode for gently removing these Ga atoms.

As illustrated in Figure 4, this is indeed the mechanism taken by Ir_3Ga_5 and the other 14-electron NCLs. Here, the DFT-optimized structures and CP schemes of Ir_3Ga_5, Ru_2Sn_3, and Ir_4Ge_5 are shown together with the helical path derived from our analysis of $RuGa_2$ (with adjustments made for the differing cell parameters and average magnitude of displacements of the E atoms from the channel center). In each case, the E-atom positions are closely aligned with the predicted path, with the major difference being in their spacing. The E-atom spacing is closest for $RuGa_2$ and becomes sparser with decreasing E content.

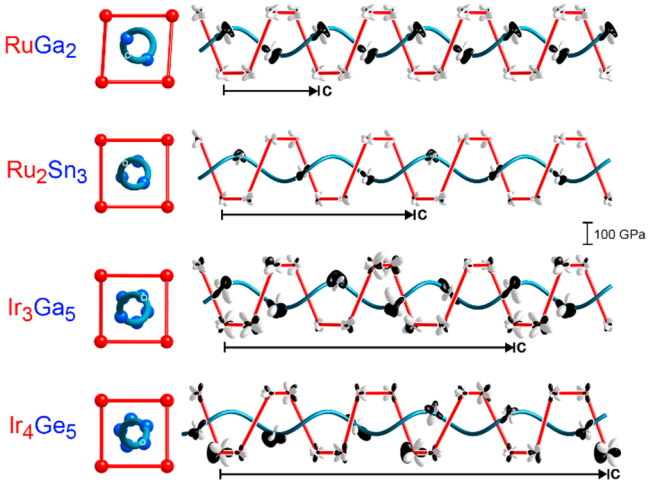

Figure 4. Placement and CP features of the main-group atoms of a series of NCL structures relative to the helical path highlighted by the CP quadrupoles in $RuGa_2$. The persistence of the CP quadrupoles suggests the presence of soft atomic motions along the path.

The CP schemes of the phases reflect these gradual structural changes. As the E atoms sample different positions along the helical path, their CP quadrupoles continue to highlight the path as a course of easy motion. In other words, the T-atom channels essentially provide continua of possible E-atom positions, consistent with the observation that incommensurate arrangements can arise when necessary to adhere to the 14-electron rule.[13] This connection could be explored further by studying how the energetics of the commensurate NCL phases change as the E atoms are shifted by different degrees along the ideal helical path—effectively exploring the energy dependence on the t_0 intercept in the (3 + 1)D model of the NCLs.[37]

In this Communication, we have illustrated how the CP scheme of the NCL parent structure reveals a well-defined path by which the T−E ratio can be tuned in response to electron-counting perturbations. The resulting picture bears commonalities with another phase we recently analyzed, Fe_2Al_5,[38] with its unusual columns of weakly ordered Al atoms.[39] In both the NCLs and Fe_2Al_5, density of states (DOS) minima emerge in the electronic structures at electron counts that optimize 18-*n* bonding schemes, but aligning the E_F with these gaps requires adjustments to the stoichiometry relative to a simple, ordered basic cell. Also, in both cases, the T-atom frameworks of the structures provide arrays of E-atom CP quadrupoles that open routes through which the structure can accommodate a range of compositions. For the NCLs, this results in an impressive series of structures, while in Fe_2Al_5, it leads to disorder and low-temperature polymorphism.[40,41]

In these systems, complex structural chemistry is heralded by two simple features that can be sought out in other intermetallics: (1) an electronic band gap or pseudogap indicating a preference for a specific electron count and (2) a sublattice of CP quadrupoles that allow facile diffusion of atoms through the structure. In such cases, the atomic packing and electronic factors in a system can respond cooperatively to electronic perturbations through new structural chemistry. We are looking forward to exploring the predictive nature of this scheme through identifying structure types with this combination of features and synthetically investigating their potential as progenitors to wider series of compounds.

■ ASSOCIATED CONTENT

Supporting Information

The Supporting Information is available free of charge on the ACS Publications website at DOI: 10.1021/acs.inorgchem.9b00132.

Computational procedures and related references, DFT-optimized geometries and total energies, phonon band structure for $RuGa_2$, and results for Ir_3Ga_5 with spin−orbit coupling (PDF)

■ AUTHOR INFORMATION

Corresponding Author

*E-mail: danny@chem.wisc.edu.

ORCID

Daniel C. Fredrickson: 0000-0002-3717-7008

Notes

The authors declare no competing financial interest.

■ ACKNOWLEDGMENTS

We thank Katerina Hilleke and Vincent Yannello for engaging discussions related to the CP and bonding schemes of the NCLs, respectively. We gratefully acknowledge financial support of the National Science Foundation (NSF) through Grants DMR-1508496 and DMR-1809594. This research involved the use of computational resources supported by NSF Grant CHE-0840494.

■ REFERENCES

(1) Oganov, A. R.; Lyakhov, A. O.; Valle, M. How Evolutionary Crystal Structure Prediction Works—and Why. *Acc. Chem. Res.* **2011**, *44*, 227−237.

(2) Zurek, E.; Grochala, W. Predicting Crystal Structures and Properties of Matter under Extreme Conditions via Quantum

DOI: 10.1021/acs.inorgchem.9b00132
Inorg. Chem. 2019, 58, 4063−4066

Mechanics: the Pressure is On. *Phys. Chem. Chem. Phys.* **2015**, *17*, 2917−2934.
(3) Zhao, X.; Nguyen, M. C.; Zhang, W. Y.; Wang, C. Z.; Kramer, M. J.; Sellmyer, D. J.; Li, X. Z.; Zhang, F.; Ke, L. Q.; Antropov, V. P.; Ho, K. M. Exploring the Structural Complexity of Intermetallic Compounds by an Adaptive Genetic Algorithm. *Phys. Rev. Lett.* **2014**, *112*, 045502.
(4) Oliynyk, A. O.; Mar, A. Discovery of Intermetallic Compounds from Traditional to Machine-Learning Approaches. *Acc. Chem. Res.* **2018**, *51*, 59−68.
(5) Ryan, K.; Lengyel, J.; Shatruk, M. Crystal Structure Prediction via Deep Learning. *J. Am. Chem. Soc.* **2018**, *140*, 10158−10168.
(6) Hyde, B. G.; Andersson, S. *Inorganic Crystal Structures*; Wiley: New York, 1989.
(7) Nowotny, H. Crystal Chemistry of Transition Element Defect Silicides and Related Compounds. In *Chemistry of Extended Defects in Nonmetallic Solids*; Eyring, L., O'Keeffe, M., Eds.; North-Holland Publishing Company: Amsterdam, The Netherlands, 1970; pp 223−237.
(8) Lidin, S.; Rohrer, F. E.; Lind, H.; Eriksson, L.; Larsson, A. K. On the Question of Commensurability - The Nowotny Chimney-Ladder Structures Revisited. *Z. Kristallogr. - Cryst. Mater.* **2000**, *215*, 650−660.
(9) Rohrer, F. E.; Lind, H.; Eriksson, L.; Larsson, A. K.; Lidin, S. Incommensurately Modulated Nowotny Chimney-Ladder Phases: $Cr_{1-x}Mo_xGe_{\sim 1.75}$ with x = 0.65 and 0.84. *Z. Kristallogr. - Cryst. Mater.* **2001**, *216*, 190−198.
(10) Sun, J.; Lee, S.; Lin, J. Four-Dimensional Space Groups for Pedestrians: Composite Structures. *Chem. - Asian J.* **2007**, *2*, 1204−1229.
(11) Jeitschko, W.; Holleck, H.; Nowotny, H.; Benesovsky, F. Die Verbindungen RuGa und $RuGa_2$. *Monatsh. Chem.* **1963**, *94*, 838−840.
(12) Völlenkle, H.; Wittmann, A.; Nowotny, H. Die Kristallstrukturen von $Rh_{10}Ga_{17}$ und Ir_3Ga_5. *Monatsh. Chem.* **1967**, *98*, 176−183.
(13) Lu, G.; Lee, S.; Lin, J.; You, L.; Sun, J.; Schmidt, J. T. $RuGa_vSn_w$ Nowotny Chimney Ladder Phases and the 14-Electron Rule. *J. Solid State Chem.* **2002**, *164*, 210−219.
(14) Jeitschko, W.; Parthé, E. The Crystal Structure of $Rh_{17}Ga_{22}$, an Example of a New Kind of Electron Compound. *Acta Crystallogr.* **1967**, *22*, 417−430.
(15) Pearson, W. Phases with Nowotny Chimney-Ladder Structures Considered as 'Electron' Phases. *Acta Crystallogr., Sect. B: Struct. Crystallogr. Cryst. Chem.* **1970**, *26*, 1044−1046.
(16) Fredrickson, D. C.; Lee, S.; Hoffmann, R. The Nowotny Chimney Ladder Phases: Whence the 14 Electron Rule? *Inorg. Chem.* **2004**, *43*, 6159−6167.
(17) Fredrickson, D. C.; Lee, S.; Hoffmann, R.; Lin, J. The Nowotny Chimney Ladder Phases: Following the c_{pseudo} Clue toward an Explanation of the 14 Electron Rule. *Inorg. Chem.* **2004**, *43*, 6151−6158.
(18) Pecheur, P.; Toussaint, G. Electronic Structure of Ru_2Si_3. *MRS Online Proc. Libr.* **1991**, *234*, 157−164.
(19) Wolf, W.; Bihlmayer, G.; Blügel, S. Electronic Structure of the Nowotny Chimney-Ladder Silicide Ru_2Si_3. *Phys. Rev. B: Condens. Matter Mater. Phys.* **1997**, *55*, 6918−6926.
(20) Filonov, A. B.; Migas, D. B.; Shaposhnikov, V. L.; Dorozhkin, N. N.; Borisenko, V. E.; Heinrich, A.; Lange, H. Electronic Properties of Isostructural Ruthenium and Osmium Silicides and Germanides. *Phys. Rev. B: Condens. Matter Mater. Phys.* **1999**, *60*, 16494−16498.
(21) Migas, D. B.; Miglio, L.; Shaposhnikov, V. L.; Borisenko, V. E. Structural, Electronic and Optical Properties of Ru_2Si_3, Ru_2Ge_3, Os_2Si_3 and Os_2Ge_3. *Phys. Status Solidi B* **2002**, *231*, 171−180.
(22) Imai, Y.; Watanabe, A. Consideration of the Validity of the 14 Valence Electron Rule for Semiconducting Chimney-Ladder Phase Compounds. *Intermetallics* **2005**, *13*, 233−241.
(23) Hayward, M. A.; Ramirez, A. P.; Cava, R. J. Structure, Stoichiometry, and Properties of the Chimney-Ladder Phases Ru_2Ge_{3+x} ($0 < x < 1$). *J. Solid State Chem.* **2002**, *166*, 389−394.
(24) Kishida, K.; Ishida, A.; Tanaka, K.; Inui, H. Thermoelectric Properties of Ru_2Si_3-based Chimney-Ladder Phases. *Mater. Sci. Forum* **2007**, *561*−*565*, 463−466.
(25) Kishida, K.; Ishida, A.; Koyama, T.; Harada, S.; Okamoto, N. L.; Tanaka, K.; Inui, H. Thermoelectric Properties of Ternary and Al-containing Quaternary $Ru_{1-x}Re_xSi_y$ Chimney−Ladder Compounds. *Acta Mater.* **2009**, *57*, 2010−2019.
(26) Sato, N.; Ouchi, H.; Takagiwa, Y.; Kimura, K. Glass-like Lattice Thermal Conductivity and Thermoelectric Properties of Incommensurate Chimney-Ladder Compound $FeGe_\gamma$. *Chem. Mater.* **2016**, *28*, 529−533.
(27) Verchenko, V. Y.; Wei, Z.; Tsirlin, A. A.; Callaert, C.; Jesche, A.; Hadermann, J.; Dikarev, E. V.; Shevelkov, A. V. Crystal Growth of the Nowotny Chimney Ladder Phase Fe_2Ge_3: Exploring New Fe-Based Narrow-Gap Semiconductor with Promising Thermoelectric Performance. *Chem. Mater.* **2017**, *29*, 9954−9963.
(28) Higgins, J. M.; Schmitt, A. L.; Guzei, I. A.; Jin, S. Higher Manganese Silicide Nanowires of Nowotny Chimney Ladder Phase. *J. Am. Chem. Soc.* **2008**, *130*, 16086−16094.
(29) Yannello, V. J.; Fredrickson, D. C. Orbital Origins of Helices and Magic Electron Counts in the Nowotny Chimney Ladders: the $18 - n$ Rule and a Path to Incommensurability. *Inorg. Chem.* **2014**, *53*, 10627−10631.
(30) Yannello, V. J.; Fredrickson, D. C. Generality of the 18-*n* Rule: Intermetallic Structural Chemistry Explained through Isolobal Analogies to Transition Metal Complexes. *Inorg. Chem.* **2015**, *54*, 11385−11398.
(31) Berns, V. M.; Engelkemier, J.; Guo, Y.; Kilduff, B. J.; Fredrickson, D. C. Progress in Visualizing Atomic Size Effects with DFT-Chemical Pressure Analysis: From Isolated Atoms to Trends in AB_5 Intermetallics. *J. Chem. Theory Comput.* **2014**, *10*, 3380−3392.
(32) Engelkemier, J.; Berns, V. M.; Fredrickson, D. C. First-Principles Elucidation of Atomic Size Effects Using DFT-Chemical Pressure Analysis: Origins of $Ca_{36}Sn_{23}$'s Long-Period Superstructure. *J. Chem. Theory Comput.* **2013**, *9*, 3170−3180.
(33) Fredrickson, D. C. DFT-Chemical Pressure Analysis: Visualizing the Role of Atomic Size in Shaping the Structures of Inorganic Materials. *J. Am. Chem. Soc.* **2012**, *134*, 5991−5999.
(34) Hilleke, K. P.; Fredrickson, D. C. Discerning Chemical Pressure amidst Weak Potentials: Vibrational Modes and Dumbbell/Atom Substitution in Intermetallic Aluminides. *J. Phys. Chem. A* **2018**, *122*, 8412−8426.
(35) Engelkemier, J.; Fredrickson, D. C. Chemical Pressure Schemes for the Prediction of Soft Phonon Modes: A Chemist's Guide to the Vibrations of Solid State Materials. *Chem. Mater.* **2016**, *28*, 3171−3183.
(36) Kilduff, B. J.; Fredrickson, D. C. Chemical Pressure-Driven Incommensurability in $CaPd_5$: Clues to High-Pressure Chemistry Offered by Complex Intermetallics. *Inorg. Chem.* **2016**, *55*, 6781−6793.
(37) van Smaalen, S. *Incommensurate Crystallography*; Oxford University Press: Oxford, U.K., 2007.
(38) Vinokur, A. I.; Hilleke, K. P.; Fredrickson, D. C. Principles of Weakly Ordered Domains in Intermetallics: The Cooperative Effects of Atomic Packing and Electronics in Fe_2Al_5. *Acta Crystallogr., Sect. A: Found. Adv.* **2019**, *75*, 297−306.
(39) Burkhardt, U.; Grin, Y.; Ellner, M.; Peters, K. Structure Refinement of the Iron-Aluminium Phase with the Approximate Composition Fe_2AI_5. *Acta Crystallogr., Sect. B: Struct. Sci.* **1994**, *50*, 313−316.
(40) Okamoto, N. L.; Okumura, J.; Higashi, M.; Inui, H. Crystal structure of η'-Fe_3Al_8; low-temperature phase of η-Fe_2Al_5 accompanied by an ordered arrangement of Al atoms of full occupancy in the c-axis chain sites. *Acta Mater.* **2017**, *129*, 290−299.
(41) Becker, H.; Leineweber, A. Atomic Channel Occupation in Disordered η-Al_5Fe_2 and in Two of its Low-temperatures Phases, η'' and η'''. *Intermetallics* **2018**, *93*, 251−262.

DOI: 10.1021/acs.inorgchem.9b00132
Inorg. Chem. 2019, 58, 4063−4066